

Organization of β -adrenoceptor signaling compartments by sympathetic innervation of cardiac myocytes

Olga G. Shcherbakova,¹ Carl M. Hurt,¹ Yang Xiang,¹ Mark L. Dell'Acqua,² Qi Zhang,¹ Richard W. Tsien,¹ and Brian K. Kobilka¹

¹Department of Molecular and Cellular Physiology, Stanford University, Stanford, CA 95305

²Department of Pharmacology, University of Colorado at Denver and Health Sciences Center, Aurora, CO 80045

The sympathetic nervous system regulates cardiac function through the activation of adrenergic receptors (ARs). β_1 and β_2 ARs are the primary sympathetic receptors in the heart and play different roles in regulating cardiac contractile function and remodeling in response to injury. In this study, we examine the targeting and trafficking of β_1 and β_2 ARs at cardiac sympathetic synapses *in vitro*. Sympathetic neurons form functional synapses with neonatal cardiac myocytes in culture. The myocyte membrane develops into specialized zones that

surround contacting axons and contain accumulations of the scaffold proteins SAP97 and AKAP79/150 but are deficient in caveolin-3. The β_1 ARs are enriched within these zones, whereas β_2 ARs are excluded from them after stimulation of neuronal activity. The results indicate that specialized signaling domains are organized in cardiac myocytes at sites of contact with sympathetic neurons and that these domains are likely to play a role in the subtype-specific regulation of cardiac function by β_1 and β_2 ARs *in vivo*.

Introduction

The sympathetic nervous system regulates cardiovascular function through innervation of the heart, kidney, and blood vessels throughout the body. Sympathetic neurons deliver catecholamines to target tissues, and the adrenal gland releases catecholamines into circulating blood. Although sympathetic nerves are the principal source of catecholamines for cardiac adrenergic receptors (ARs), little is known about the cell–cell interactions between sympathetic nerves and cardiac myocytes.

β_1 and β_2 ARs, which are members of the G protein-coupled receptor (GPCR) family, form the interface between the sympathetic nervous system and cardiac muscle. However, the function and distribution of specific β AR subtypes at cardiac sympathetic synapses have not been addressed. These homologous receptors play distinct roles in regulating normal cardiovascular physiology (Rohrer et al., 1999), and there is a growing body of evidence that they play opposing roles in the pathogenesis of heart failure (Patterson et al., 2004; Bernstein

et al., 2005; Zheng et al., 2005). A better understanding of the subtype-specific signaling of β_1 and β_2 ARs in cardiac myocytes in response to sympathetic nervous system activation could have implications for the prevention and treatment of heart failure.

β_1 and β_2 ARs are highly homologous both structurally and functionally. They share 52% identity overall and 76% identity in the transmembrane domains. However, studies in both neonatal and adult cardiac myocytes provide compelling evidence that β_1 and β_2 ARs signal through distinct pathways (Xiang and Kobilka, 2003b; Xiao et al., 2004). In neonatal myocytes, activated β_1 AR couples only to Gs (guanine nucleotide-binding protein that stimulates adenylyl cyclase) and leads to a PKA-dependent increase in the contraction rate. In contrast, activated β_2 AR undergoes sequential coupling to Gs and Gi (guanine nucleotide-binding protein that inhibits adenylyl cyclase), having a biphasic effect on the contraction rate that is independent of PKA activation (Devic et al., 2001).

Functional differences between β_1 and β_2 ARs in cardiac myocytes can be attributed to subtype-specific targeting to different signaling compartments in the myocyte plasma membrane (Xiang et al., 2002). Activated β_2 ARs undergo robust endocytosis, whereas activated β_1 ARs remain at the plasma membrane (Xiang et al., 2002). In neonatal cardiac myocytes,

Correspondence to Brian Kobilka: kobilka@stanford.edu

Y. Xiang's current address is Department of Molecular and Integrative Physiology, University of Illinois at Urbana-Champaign, Urbana, IL 61801.

Abbreviations used in this paper: AR, adrenergic receptor; GPCR, G protein-coupled receptor; KO, knockout; nAChR, nicotinic acetylcholine receptor; SGN, sympathetic ganglion neuron.

The online version of this article contains supplemental material.

endocytosis and recycling are both required for the switch in β_2 AR coupling from Gs to Gi (Devic et al., 2001; Shenoy and Lefkowitz, 2003; Xiang and Kobilka, 2003b). β_2 ARs are predominantly concentrated in caveolar structures, whereas β_1 ARs are mainly distributed in the noncaveolar membrane (Rybin et al., 2000). The cAMP phosphodiesterase PDE4D regulates signaling by the β_2 AR but has no detectable effect on β_1 AR signaling, suggesting that this phosphodiesterase isoform might be a component of the β_2 AR signaling complex (Xiang et al., 2005). These observations suggest that distinct signaling domains exist in cardiac myocytes to conduct β_1 and β_2 AR signaling.

The heart is richly innervated by sympathetic neurons, which are the principal source of catecholamines for cardiac ARs (Armour, 1994). As β_1 and β_2 ARs are the primary sympathetic receptors in the heart, their distribution and function could be influenced by the sympathetic innervation of cardiac myocytes. Synapses in the central nervous system and neuromuscular junctions are formed by coordinated assembly and tight attachment of pre- and postsynaptic specializations (Sanes and Lichtman, 2001). At the site of contact, the postsynaptic plasma membrane develops into a specialized zone that contains accumulations of neurotransmitter receptors, channels, and anchoring and signaling molecules (Sheng and Kim, 2002). This colocalization is thought to provide a fast and efficient response to released neurotransmitter. Accumulation of receptors at the postsynaptic sites is regulated by synaptogenesis, whereas the dynamic behavior of receptors, such as endocytosis, exocytosis, and lateral movement, is regulated by activity-dependent cues (Misgeld et al., 2002; Brecht and Nicoll, 2003; Park et al., 2004; Perez-Otano and Ehlers, 2005).

In this study, we report the first detailed analysis of the organization of signaling molecules at the site of innervation of cardiac myocytes by sympathetic neurons. We demonstrate that sympathetic ganglion neurons (SGNs) regulate the contraction rate of cultured myocytes and provide evidence that sympathetic innervation influences the structure of the myocyte membrane and the organization and distribution of β_1 and β_2 AR signaling compartments. Cardiac myocytes induce presynaptic differentiation in contacting axons; synaptic vesicles accumulate at the sites of contact as delineated by synapsin I. On the postsynaptic side, the myocyte membrane develops into specialized zones that surround contacting axons and contain accumulations of the scaffold proteins SAP97 and AKAP79/150. In contrast, staining for caveolin-3, which is a marker of signaling caveolae microdomains in cardiac myocytes, is diminished at the sites of contact. The cardiac myocyte membranes are linked to contacting neurons by cadherin-catenin complexes. We have found striking differences in the trafficking of β_1 and β_2 AR-expressed myocytes that have been innervated by cultured sympathetic neurons. β_1 ARs accumulate at the synaptic zones, whereas β_2 ARs undergo local internalization from the synaptic sites in a neuronal activity-dependent manner. The subtype-specific differences in the localization of β_1 and β_2 AR at sympathetic synapses likely contribute to the regulation of cardiac performance by the sympathetic nervous system in vivo.

Results

SGNs form functional connections with cardiac myocytes in vitro

To determine whether SGNs form functional connections with neonatal cardiac myocytes in vitro, we stimulated the cardiac myocyte contraction rate through the activation of neurons. The sympathetic cervical (autonomic) ganglia contain predominantly neuronal nicotinic acetylcholine receptors (nAChRs), which play a central role in neural transmission in the autonomic nervous system. In vivo, the transmitter released from the preganglionic axon terminals is primarily acetylcholine, which depolarizes postsynaptic neurons by the activation of nAChR (Haass and Kubler, 1997; Lechner et al., 2003). The activation of nAChR with nicotine causes the depolarization of SGN, which, in turn, triggers neurotransmitter release. It has been shown that nicotine-induced changes in the heart rate are associated with an increase in plasma catecholamine concentrations, and they are attenuated by β AR blockade, indicating that the increase in heart rate is mediated by β ARs (Haass and Kubler, 1997). Nicotine applied to cardiac myocytes in the absence of neurons did not produce any changes in the contraction rate (unpublished data).

Myocytes were cocultured on the same coverslip with SGN or on separate coverslips (Fig. 1). SGNs were stimulated with 1 μ M nicotine. This relatively low concentration of nicotine was used to minimize the release of catecholamines into the media because it has been shown that nicotine concentrations

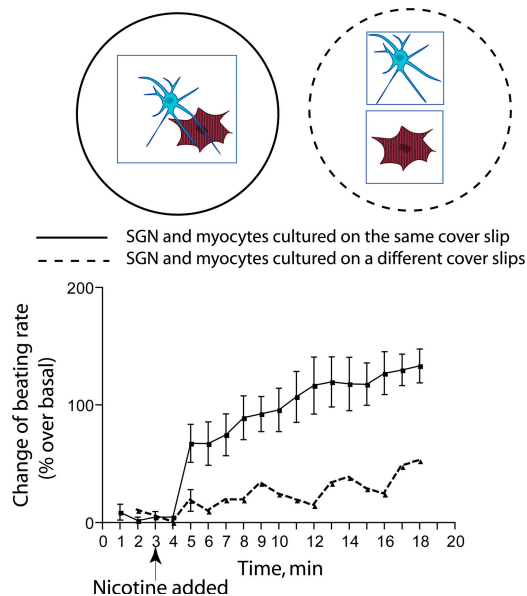


Figure 1. Stimulation of SGNs by nicotine results in an increase in the beating rate of contacting myocytes. Myocytes and SGNs were cocultured on the same coverslip or on separate coverslips in the same culture dish. The change in myocyte contraction rate was monitored by video microscopy before and after the stimulation of SGNs with 1 μ M nicotine tartrate. The data are the mean \pm SEM (error bars) of three experiments. Two-way analysis of variance demonstrated that there was a significantly greater increase in the beat rate of myocytes cocultured on the same coverslip with SGNs compared with myocytes and neurons cultured on separate coverslips ($P < 0.0001$). The increase of the beat rate over baseline was significant for both curves ($P < 0.001$).

over 3 μM can lead to an accumulation of noradrenaline in the media of cultured SGNs (Norenberg et al., 2001). We observed an increase (~ 2.5 -fold) in the contraction rate of cardiac myocytes cultured on the same coverslip with SGN (Fig. 1). The effect was much lower when myocytes and neurons were placed on different coverslips and, therefore, could not form connections with each other. Thus, stimulation of the myocyte contraction rate by activated SGNs requires that neurons form contacts with myocytes.

Formation of specialized cell-cell contacts between cardiac myocytes and SGNs

Accumulation of synapsin I in axons that contact myocytes. Synaptogenesis involves the organization of specialized signaling complexes at sites of cell-cell contact that are designed to rapidly and efficiently relay signals from one cell to another (Garner et al., 2002). To test whether cardiac myocytes induce the formation of active presynaptic zones in contacting

axons, we immunostained the cocultures with an antibody to synapsin I, a peripheral membrane protein of synaptic vesicles (Scheiffele et al., 2000). We observed the formation of synapsin I puncta in axons contacting cardiac myocytes, which suggests that synaptic vesicles cluster at those sites (Fig. 2, A and C). The accumulation of synapsin I increased with the time of coculturing cardiac myocytes and SGNs (unpublished data). In contrast, the accumulation of synapsin I was much less pronounced in neurons that contacted cardiac fibroblasts stained for fibronectin (Fig. 2, B and C). Particularly notable was the difference in the number of large ($>1 \mu\text{M}$) puncta of synapsin I, which was greater in myocytes compared with fibroblasts. This suggests that neurons form specialized contacts with myocytes.

Synaptic vesicles undergo activity-dependent recycling at the sites of contact of cardiac myocytes and SGNs. Synapsin accumulation may not necessarily mark functional sites of transmitter release. To examine synaptic activity, we monitored activity-dependent internalization of an antibody to the luminal domain of synaptotagmin, a method that has been shown to mark the sites of synaptic vesicle endocytosis (Kraszewski et al., 1995). Synaptotagmin antibody was added to cocultures of myocytes and SGNs, and antibody internalization was stimulated by the addition of 500 μM nicotine. Cultures were then fixed and costained for synapsin I (Fig. 3). Synaptotagmin antibody internalization colocalizes with synapsin I throughout the axon. The uptake was completely abolished in Ca^{2+} -free media. Therefore, synaptic vesicles undergo activity-dependent recycling at the sites of contact of SGNs and cardiac myocytes.

We also performed analysis of the activity-dependent destaining of FM1-43 dye. The fluorescent styryl dye FM1-43 is taken up by synaptic vesicles in an activity-dependent manner (Betz and Bewick, 1992; Ryan et al., 1993; Zakharenko et al., 2001). Cocultures were loaded with FM1-43 in the presence of 500 μM nicotine for 5 min and were washed to remove background staining (Fig. S1 A, available at <http://www.jcb.org/cgi/content/full/jcb.200604167/DC1>). During a second round of nicotine stimulation, the fluorescence intensity of labeled puncta rapidly diminished by $\sim 80\%$, reflecting exocytosis of the dye from synaptic vesicles (Fig. S1, B and C). Therefore, synaptic vesicles undergo activity-dependent recycling at the sites of contact of SGNs and cardiac myocytes. As with the antibody to the luminal domain of synaptotagmin, FM1-43 uptake is punctate and is not uniformly distributed along the axon. Therefore, it is likely that release occurs at closely spaced but discrete sites along the entire axonal contact.

Exclusion of caveolin-3 at sites of contact between myocytes and SGNs. Caveolin-3 is expressed in cardiac myocytes and marks specialized membrane microdomains known as caveolae; thus, we have used caveolin-3 as a cardiac myocyte-specific marker. Previous studies showed that $\beta_2\text{ARs}$ are associated with caveolin-3 in the neonatal cardiac myocyte and that this localization may be important for physiologic function (Devic et al., 2001; Xiang et al., 2002). Interestingly, we observed the exclusion of caveolin-3 from membranes of cardiac myocytes at sites of contact with neurons in

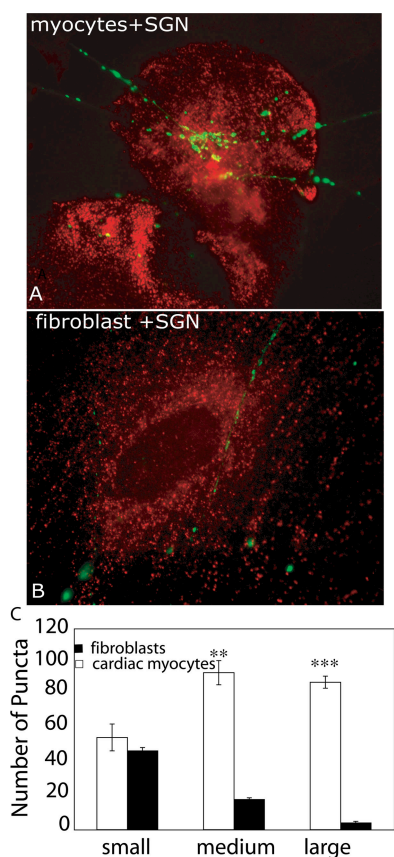


Figure 2. Accumulation of synapsin at contact sites of SGNs and cardiac myocytes. (A) SGNs and cardiac myocytes at 9 d in coculture immunostained with an antibody to synapsin I (green) and caveolin-3 (red). (B) SGNs and cardiac fibroblasts at 9 d in coculture stained with antibody to synapsin I (green) and fibronectin (red). (C) Quantitative comparison of synapsin puncta formation in cocultures of SGNs and cardiac myocytes versus SGNs and cardiac fibroblasts. The number of puncta on 10 cells averaged over three experiments. The approximate sizes of synapsin I puncta were as follows: large, $>1.0 \mu\text{m}$; medium, $0.5\text{--}1.0 \mu\text{m}$; small, $<0.5 \mu\text{m}$ ($n = 15$ cells). A t test was used to determine significance (**, $P < 0.01$ for medium puncta; ***, $P < 0.001$ for large puncta). Error bars represent SEM.

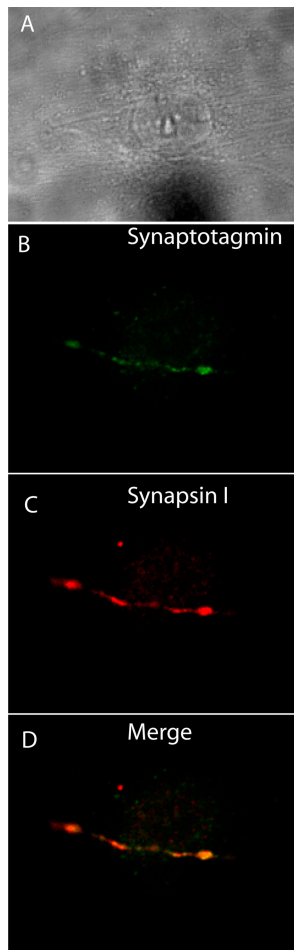


Figure 3. Visualization of active synaptic sites in a coculture of cardiac myocytes and SGNs by uptake of an antibody to the luminal domain of synaptotagmin. A coculture of cardiac myocytes and SGNs was incubated with serum-free media containing 500 μ M nicotine and 10 μ g/ml rabbit polyclonal antibody to the luminal domain of synaptotagmin for 15 min followed by rinsing, fixation, and immunostaining with a mouse monoclonal antibody to synapsin I. (A) Brightfield image of the coculture. (B) Immunostaining for synaptotagmin (green). (C) Immunostaining for synapsin I (red). (D) Merged image of B and C.

~60% of cells examined by two-photon microscopy (Fig. 4). The loss of caveolin-3 is not limited to sites adjacent to synapsin I accumulation but extends through the length of the axon. We did not observe an increase in the removal of caveolin-3 after stimulation of the cocultures with nicotine, suggesting that caveolin-3 may be excluded from the myocyte membrane upon the formation of contacts with SGN. Caveolin marks plasma membrane signaling domains that recruit certain lipid-modified membrane proteins (including receptors, G proteins, and tyrosine kinases) while excluding other proteins and lipid components (Cohen et al., 2004). Removal of caveolin-3 from the contact sites of myocytes and neurons indicates a reorganization of signaling microdomains in the plasma membrane of cardiac myocytes in contact with SGN axons.

Cadherin-catenin complexes form at the sites of contact between cardiac myocytes and SGNs. Cadherins are calcium-dependent homophilic cell adhesion molecules that maintain the integrity of cell-cell

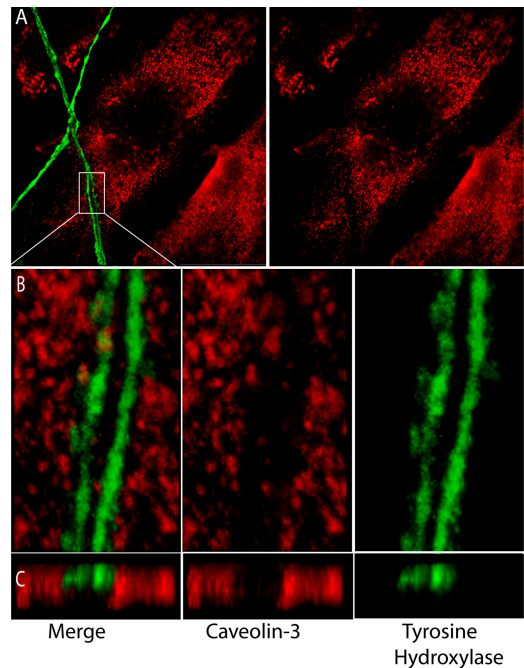


Figure 4. Caveolin-3 is diminished at sites of contact between cardiac myocytes and SGNs. (A) Cardiac myocytes and SGNs at 9 d in coculture were immunostained with antibodies for caveolin-3 (red) and tyrosine hydroxylase (green) and were imaged by two-photon microscopy. (B) 3D reconstruction of an enlarged region of the boxed image in A. (C) X-z cross section of the 3D reconstruction.

junctions and promote the stability of synapses by linking pre- and postsynaptic membranes. Extracellular domains of cadherins interact directly to help hold the membranes of two cells together. The requirement of mechanical stability is most clear at the neuromuscular junction, which is maintained in the face of constant mechanical stress from muscle contraction (Yamagata et al., 2003). We observed puncta of pancadherin immunostaining on the surface of cardiac myocytes localized along traces of axons, which were identified by staining with an antibody to tyrosine hydroxylase (Fig. 5 A). As shown on a two-photon image (Fig. 5 C), synapsin I puncta were often observed overlapping cadherin immunostaining (frequency of $74 \pm 15\%$ [SEM]). However, cadherin puncta are more abundant, and the majority of cadherin staining does not localize with synapsin I puncta. Nevertheless, cadherin puncta are not observed in myocytes cultured in the absence of SGN (unpublished data), suggesting that these puncta represent contacts between SGN fibers and myocytes. The fact that not all cadherin staining localizes with synapsin I puncta suggests that not all contacts between SGNs and myocytes are sites of synaptic activity.

Cadherins are known to form complexes with β -catenin, which, in turn, associates with α -catenin and the actin cytoskeleton. Immunostaining of cocultures for synapsin I and β -catenin revealed that the pattern of staining for β -catenin (Fig. 6) was very similar to the pattern of staining for pancadherin (Fig. 5), and the majority of synapsin I puncta colocalized with β -catenin (Fig. 6, C–E). Our culture results predict that catenin-cadherin complexes may be important for stabilizing interactions between myocytes and neurons in vivo. Therefore, we examined the

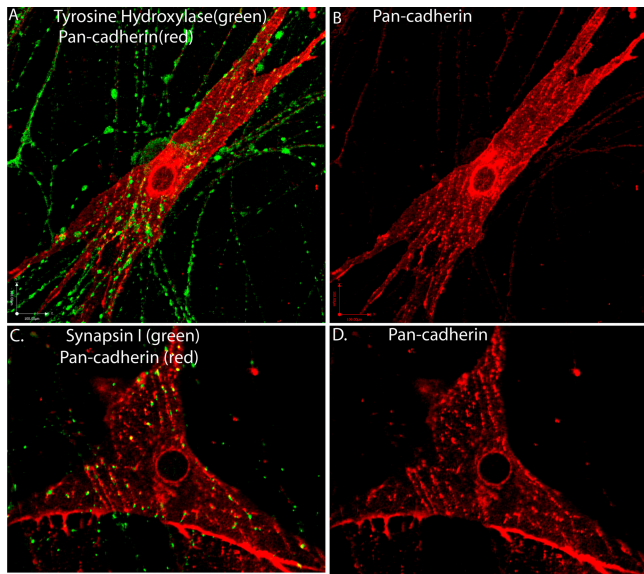


Figure 5. Cadherins accumulate at sites of contact between cardiac myocytes and SGNs. (A) Cardiac myocytes and SGNs at 5 d in coculture were immunostained for tyrosine hydroxylase (green) and pancadherin (red). (B) Same image as in A showing only pancadherin immunostaining. (C) Cardiac myocytes and SGNs at 5 d in coculture were immunostained for synapsin I (green) and pancadherin (red). (D) Same image as in C showing only pancadherin immunostaining.

distribution of β -catenin relative to synapsin I in intact ventricular muscle from the mouse heart. Tissue sections were stained with antibodies to synapsin I and β -catenin and were examined by two-photon microscopy. Consistent with our culture results, we observed the accumulation of β -catenin surrounding contacting axons (Fig. S2, available at <http://www.jcb.org/cgi/content/full/jcb.200604167/DC1>). These results suggest that cadherin–catenin complexes may be involved in stabilizing interactions between SGNs and myocytes *in vivo*; however, we have no evidence that they play a direct role in synaptic function.

Subtype-specific targeting and trafficking of β_1 and β_2 ARs at sympathetic synapses in cardiac myocytes

Collectively, the aforementioned data demonstrate that in coculture, cardiac myocytes and SGNs form specialized functional connections. Catecholamines (epinephrine and predominantly norepinephrine) are the major neurotransmitters released from SGN (Esler and Kaye, 2000), and β ARs are the principal catecholamine receptors in cardiac myocytes. Therefore, we examined how interactions with SGN fibers and neurotransmission affect the localization of β ARs in myocytes. Currently available antibodies are not adequate to detect endogenous β ARs in cardiac myocytes. Thus, to visualize β_1 and β_2 ARs in cardiac myocytes, we expressed FLAG-tagged β_2 AR or HA-tagged β_1 AR via recombinant adenovirus in cocultures. We have previously shown that the functions of epitope-tagged β_1 and β_2 ARs expressed in β_1 AR/ β_2 AR knockout (KO) myocytes are indistinguishable from endogenous receptors in β_2 AR KO and β_1 AR KO myocytes, respectively (Xiang et al., 2002; Xiang and Kobilka, 2003a). We took advantage of the fact that SGNs at 7–10 d in

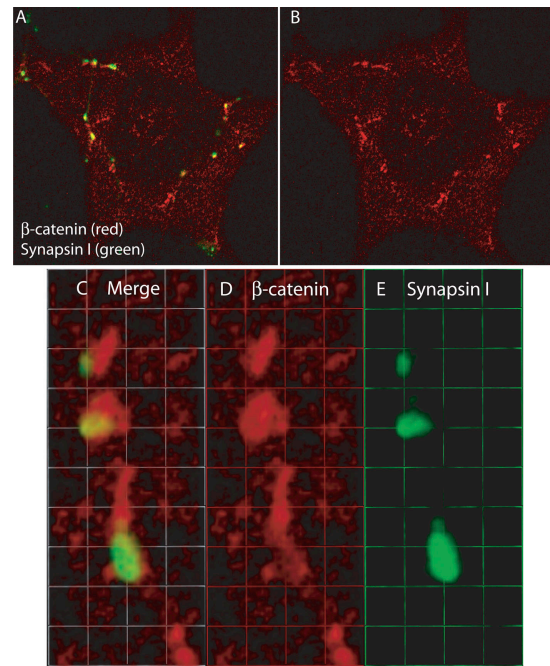


Figure 6. β -catenin accumulation at sites of contact between cardiac myocytes and SGNs. (A) Cardiac myocytes were cocultured with SGNs for 2 d, immunostained for β -catenin (red) and synapsin I (green), and imaged by two-photon microscopy. (B) Same image as in A showing only β -catenin immunostaining. (C–E) 3D-reconstructed enlarged fragment from A. 1 U = 1.4 μ m.

culture are highly resistant to adenovirus infection; therefore, we were able to express the receptors predominantly in cardiac myocytes and analyze the distribution of β ARs relative to synaptic sites. To address activity-dependent events in cocultures, we stimulated neurotransmission through activation of the nAChRs of SGN with 500 μ M nicotine.

β_2 ARs are removed from synaptic sites after SGN stimulation. We observed no changes in the distribution of FLAG-tagged β_2 AR in the majority of cardiac myocytes in contact with unstimulated SGNs (Fig. 7, A and B). However, in a few cells per coverslip (\sim 1–2%), we observed a decrease in FLAG antibody staining at sites of SGN–myocyte contacts (Fig. 7, C and D). Nicotine induced the removal of FLAG-tagged β_2 ARs from the surface of cardiac myocytes at the sites of contact with SGNs (Fig. 7, E–H). This effect was observed in $72 \pm 6\%$ of myocytes in nicotine-stimulated cocultures. β_2 AR removal was observed in only $15 \pm 2\%$ of myocytes from nicotine-stimulated cultures pretreated with the β AR antagonist alprenolol (Fig. S3, available at <http://www.jcb.org/cgi/content/full/jcb.200604167/DC1>), indicating that the trafficking of β_2 ARs requires activation of the receptor. We observed the effect as fast as 5 min after the treatment, which is consistent with the time course of the activation of cardiac myocytes through neurons described earlier (Fig. 1). The time course of the removal of β_2 AR is also consistent with the time course of β_2 AR activation and internalization (von Zastrow and Kobilka, 1992). Thus, we concluded that β_2 ARs are locally internalized at the sites of contacts, and this redistribution is regulated by neuronal activity.

Quantitation of β_2 AR staining intensity revealed a significant decrease in intensity along the trace of axons marked by

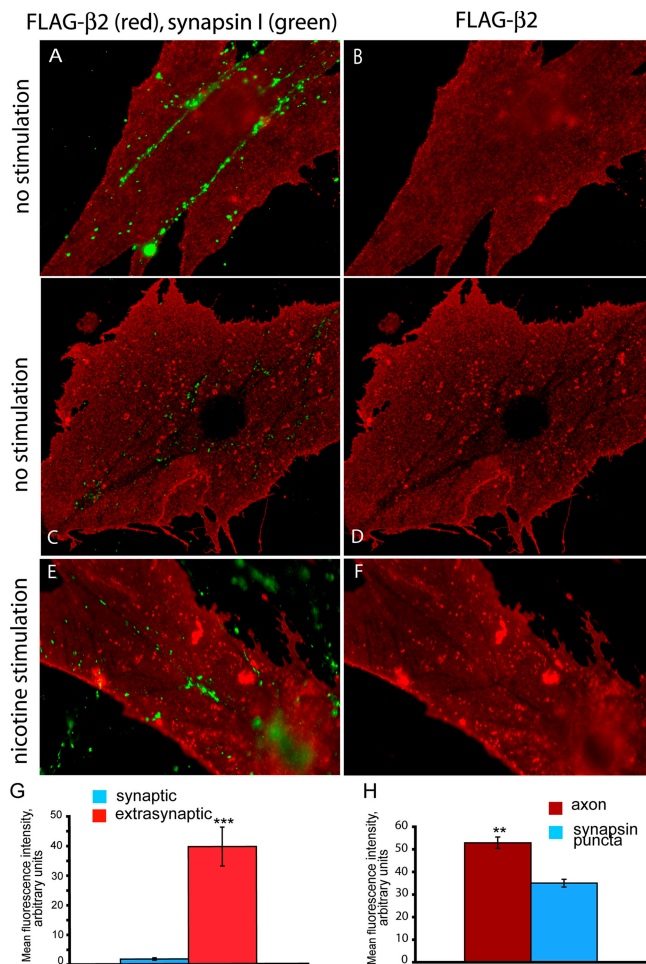


Figure 7. β_2 AR is depleted at synaptic sites after stimulation of neuronal activity. Cardiac myocytes were cocultured with SGNs for 6 d, infected with recombinant adenovirus expressing FLAG-tagged β_2 AR, and cultured for an additional 48–72 h before immunostaining for FLAG (red) and synapsin I (green). (A and B) Nonstimulated cultures. (C and D) Example of β_2 AR removal by spontaneous neuronal activity in nonstimulated coculture. (E and F) Cocultures that were stimulated with 500 μ M nicotine for 5 min. (G) Comparison of the fluorescence intensity of immunostaining for FLAG-tagged β_2 AR in synaptic and extrasynaptic areas after the stimulation of coculture with nicotine. The mean fluorescence intensity for the red channel representing immunostaining for FLAG-tagged β_2 AR was measured in areas where the green channel fluorescence (immunostaining for synapsin I) was selected as a criterion. Next, we excluded the area selected and measured the fluorescence for the red channel at extrasynaptic regions. Data were collected from 10 images obtained in three experiments. (H) Comparison of the fluorescence intensity of immunostaining for FLAG-tagged β_2 AR beneath synapsin I puncta and between synapsin I puncta along the axon after the stimulation of coculture with nicotine. To compare the fluorescence intensity of β_2 AR staining in the areas of synapsin I accumulation with areas along axons between synapsin I puncta, we used the Wizard tool of the Volocity program to select regions of interest. Data were obtained from three images using six different pairs of the region of interest on each image. (G and H) Measurements were performed in arbitrary units of the direct scale. Comparisons were performed with a *t* test. Statistical significance was set as $P < 0.05$. **, $P < 0.01$; ***, $P < 0.001$.

synapsin I staining compared with areas of the myocyte not in contact with axons ($P < 0.05$; Fig. 7 G). We also found that β_2 AR staining intensity was significantly lower under synapsin I staining puncta compared with regions along SGN axons that lie between synapsin I puncta ($P < 0.05$; Fig. 7 H). These data

suggest that the release of transmitter is not uniform along the contacting axons and are consistent with antisynaptotagmin antibody and FM1-43 uptake experiments (Figs. 3 and S1).

β_1 ARs are localized to zones of myocyte-SGN contact. The pattern of β_1 AR distribution is strikingly different from that of the β_2 AR (Fig. 8, A–G). In cocultures immunostained for synapsin I and HA-tagged β_1 AR, we observed approximately two times more staining for HA-tagged β_1 ARs in myocyte membrane associated with axonal traces compared with myocyte membrane not associated with axons (Fig. 8 H). The immunostaining pattern for HA-tagged β_1 ARs mirrors the shape of overlying axons (Fig. 8, A–D), and the maximum accumulation of the receptors often surrounds the sites of synapsin I accumulation, which are presumably the sites of highest neurotransmission activity. The characteristic zones highlighted by immunostaining for HA-tagged β_1 ARs and surrounding traces of axons on the surface of myocytes appear as soon as the second day of coculture and become much more pronounced in mature cocultures (10 d; unpublished data). Interestingly, using 3D reconstructions from two-photon z sections, we observe an invagination of the myocyte membrane at the point of contact with an SGN (Fig. 8, E–G; and Video 1, available at <http://www.jcb.org/cgi/content/full/jcb.200604167/DC1>). This suggests that cardiac myocytes change their morphology to establish functional contacts with SGNs. We did not observe an effect of nicotine or β blockers on the distribution of HA-tagged β_1 AR in cardiac myocytes. Thus, our data indicate that β_1 ARs are stable residents at sympathetic synapses, whereas the β_2 ARs undergo dynamic trafficking events regulated by neuronal activity.

Disruption of the PDZ domain of β_1 AR did not affect localization to zones of myocyte-SGN contact. We have previously observed that disruption of the PDZ-binding motif of the C terminus of β_1 AR has a dramatic effect on both trafficking and signaling in cardiac myocytes. Unlike wild-type β_1 AR, β_1 AR lacking a PDZ-binding motif (β_1 AR-PDZ) is able to undergo agonist-induced internalization and can couple to both Gs and Gi. Thus, PDZ domain interactions are important for normal β_1 AR function. Surprisingly, localization of β_1 AR-PDZ relative to sympathetic synapses was indistinguishable from wild-type β_1 AR (Fig. 8, C and D), suggesting that some other domains of β_1 AR are primarily responsible for localization of the receptor relative to the synapse.

Accumulation of scaffold molecules at zones of myocyte-SGN contact

As shown in Fig. 8 (E–G), there is an invagination of the myocyte membrane at sites of contact between cardiac myocytes and SGN cells. This bears a resemblance to the structure of neuromuscular junctions in skeletal muscle. Moreover, the subtype-specific localization of β_1 and β_2 ARs and the exclusion of caveolin-3 suggest that sites of contact between myocytes and SGNs are specialized signaling domains. Therefore, we looked for other molecules that have been associated with synapses and might be involved in the trafficking, regulation, and signaling of β_1 AR. Members of the SAP90/PSD-95 subfamily of membrane-associated guanylate kinase homologues have recently emerged as important players in the molecular organization of synapses

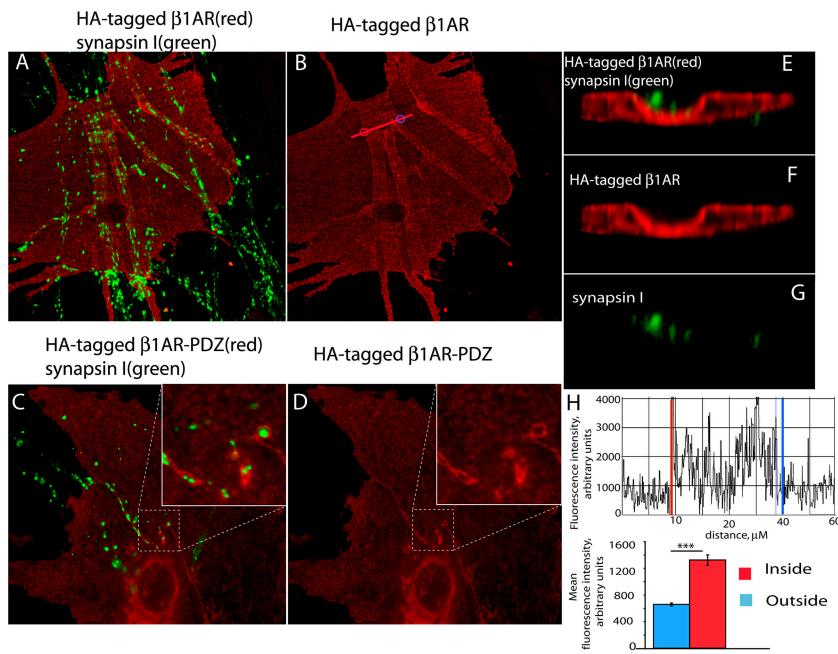


Figure 8. β_1 ARs accumulate at sites of contact between SGNs and cardiac myocytes. (A and B) Cardiac myocytes were cocultured with SGNs for 6 d, infected with recombinant adenovirus expressing HA-tagged β_1 AR, and cultured for an additional 24 h before immunostaining for HA (red) and synapsin I (green). (C and D) Cardiac myocytes were cocultured with SGNs for 6 d, infected with recombinant adenovirus expressing HA-tagged β_1 AR-PDZ, and cultured for an additional 24 h before immunostaining for HA (red) and synapsin I (green). Insets show enlargements of the images outlined by dotted white lines. (E–G) X-z cross section of the 3D reconstruction of a two-photon image of the site of contact between a cardiac myocyte expressing HA-tagged β_1 AR and an SGN immunostained for HA (red) and synapsin I (green). (H) Histogram of the fluorescence intensity along the red line in B. The red and blue lines indicate the boundaries of the axon bundle, which are represented by red and blue circles in B. (bottom) Comparison of the accumulation of β_1 AR in the zones of contact with SGNs. The histograms of fluorescence intensity of the original LSM510 files for five different images were used to quantify the accumulation of β_1 AR in the zones of contact with SGNs. The mean fluorescence intensity in the areas inside and outside the zones of contact along the selected straight line crossing a zone of contact was quantified (H; two zones from each image). Measurements were performed in arbitrary units of the direct scale. Statistic comparisons were performed with a *t* test. Error bars represent SEM. ***, *P* < 0.001.

in neurons (Funke et al., 2005). In contrast to most other membrane-associated guanylate kinase homologues, the synapse-associated protein SAP97 is also expressed in nonneuronal tissues, including cardiac myocytes (Muller et al., 1995). Indeed, we have found that SAP97 localized to the zones of contact between myocytes and SGNs (Fig. S4, available at <http://www.jcb.org/cgi/content/full/jcb.200604167/DC1>). We also examined the localization of SAP97 in intact ventricular muscle from the mouse heart. Tissue sections were stained for synapsin I and SAP97 and examined by two-photon microscopy. Consistent with our culture results, we observed the accumulation of SAP97 surrounding contacting axons (Fig. S5).

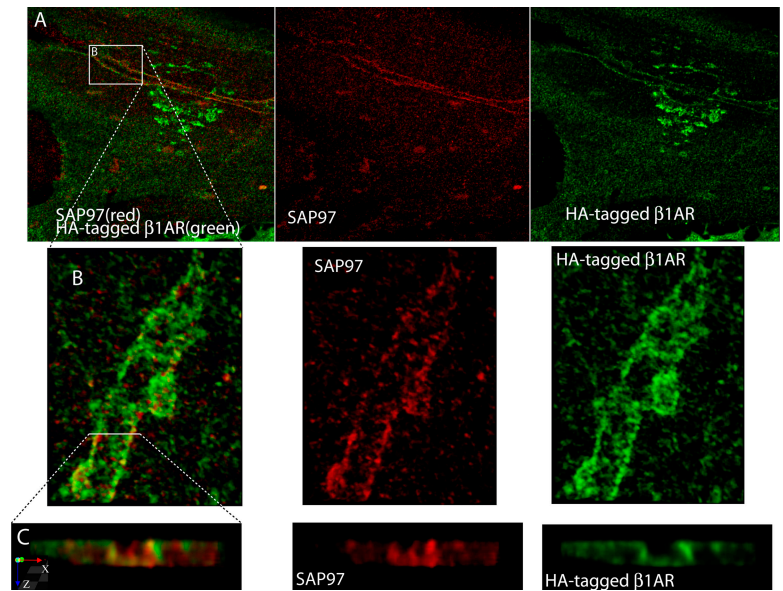
The intensity of immunostaining for SAP97 associated with SGN was increased after 90 min of stimulation with nicotine in cocultures in which β_1 AR was overexpressed in cardiac myocytes (Fig. S4). We conducted a blind analysis of the size and intensity of SAP97-positive spots (puncta). Cocultures that were stimulated by nicotine exhibited an increase in the area and intensity of SAP97-positive puncta when compared with the controls (Fig. S4, C and D). An increase in the size of SAP97-positive puncta was also observed in wild-type cardiac myocytes not expressing exogenous β_1 AR, but the increase was not statistically significant. SAP97 was observed at the synaptic sites in β_1 AR KO and β_1/β_2 AR KO myocytes, but we did not detect an increase in the intensity of immunostaining for SAP97 after nicotine stimulation. The results suggest that β_1 AR signaling can modulate SAP97 accumulation at synapses. Two-photon imaging revealed a partial overlap in immunostaining for β_1 AR and SAP97 in cardiac myocytes (Fig. 9). Thus, the proteins may function within the same signaling compartment but may not directly interact.

The postsynaptic density in neuronal synapses and postsynaptic membranes in neuromuscular junctions are known to contain accumulations of receptors, channels, and anchoring and signaling molecules. This colocalization is thought to provide a fast and efficient response to released neurotransmitter as well as facilitate retrograde signaling from targeting cells to the contacting neuron. PKA and phosphatase 2B anchored by AKAP79 are known to be associated with postsynaptic density in neurons (Dell'Acqua et al., 2002; Bauman et al., 2004), and PKA and D-AKAP are also found in and around the neuromuscular junction (Perkins et al., 2001). By analogy with this, we have found the accumulation of AKAP79/150 (mouse orthologue of AKAP79) to the zones of contact between cardiac myocytes and SGNs (Fig. 10, A and B). When we expressed HA-tagged β_1 AR in cardiac myocytes in a coculture and immunostained the cocultures for AKAP79/150 and HA, we observed both proteins at the zones of contact. Although there may be some overlap, the pattern of staining appears to be different (Fig. 10, C and D), suggesting that these proteins may not interact directly. Nevertheless, their proximity in the sympathetic synapse suggests that AKAP79/150 could play a role in β_1 AR signaling. In contrast, two other PDZ scaffold proteins known to localize to cell–cell contacts, MAGI-3 and MUPP1, were not detected at sites of myocyte–SGN contact (unpublished data).

Discussion

The sympathetic nervous system plays a central role in the cardiovascular response to acute stress by increasing heart rate and contractility. However, chronic sympathetic nervous system hyperactivity has been implicated in the pathogenesis of heart

Figure 9. **SAP97 and β_1 ARs localize to cardiac sympathetic synapses in vitro.** (A) Cardiac myocytes were cocultured with SGNs for 6 d, infected with recombinant adenovirus expressing HA-tagged β_1 AR, and cultured for an additional 24 h before immunostaining for HA (green) and SAP97 (red). Two-photon image. (B and C) Enlargements of the boxed area in A.



failure (Mann and Bristow, 2005). The assembly, development, and function of synapses between neurons in the central nervous system (Sudhof, 2001) and neuromuscular junctions of skeletal muscle (Sanes and Lichtman, 1999; Goda and Davis, 2003) have been characterized in depth. Much less is known about sympathetic synapses. In this study, we provide evidence that contact between SGN axons and myocytes leads to the formation of specialized zones in the myocyte membrane. These zones are characterized by the accumulation of β_1 ARs as well as adhesion and scaffold molecules and the exclusion of caveolin-3. The observation that there is an activity-dependent loss of β_2 AR staining at regions of synapsin I accumulation suggests that synaptogenesis takes place within these specialized SGN–myocyte contacts.

Sympathetic innervation in culture is predominantly adrenergic

Previous studies of rat cardiac myocytes cultured together with dissociated rat superior cervical ganglia show that these neurons can differentiate into adrenergic neurons and cholinergic neurons and that most cultured neurons secreted both neurotransmitters, with at least some of the acetylcholine release being at autosynapses (Furshpan et al., 1986; Potter et al., 1986). It has been shown that brain-derived neurotrophic factor alters the release properties of these cultured neurons from excitatory (adrenergic) to inhibitory (cholinergic; Yang et al., 2002). Although we observed that most cultured SGNs were positive for both cholinergic and adrenergic markers (unpublished data) in our cultures, our functional studies indicate that the neurons in contact with cardiac myocytes are predominantly adrenergic, as stimulation led to a robust increase in the intrinsic rate of spontaneously beating cardiac myocytes (Fig. 1).

Sympathetic synapses induce the formation of distinct plasma membrane signaling domains on cardiac myocyte membranes

Sympathetic synapses between cardiac myocytes and SGNs are unique cell–cell contacts designed for the efficient regulation of

heart rate and contractility by the autonomic nervous system. The mechanism for the initiation and development of cardiac sympathetic synapses is not known. Cardiac myocytes do not express MuSK (Valenzuela et al., 1995), a key organizer of the postsynaptic zones in neuromuscular junctions, suggesting that sympathetic synapse formation does not involve agrin–MuSK signaling. One of the early events observed in our studies is the formation of cadherin–catenin complexes at the sites of contact between cardiac myocytes and SGN axons. Cadherins are known to form complexes with β -catenin, which, in turn, associates with α -catenin and the actin cytoskeleton. There is a growing body of evidence that cadherin–catenin complexes function as signaling centers at neuronal synapses (Bamji et al., 2003). We observed punctate immunostaining for both pancadherin and β -catenin on the surface of cardiac myocytes localized along traces of axons (Figs. 5 A, 6, and S2). Synapsin I puncta were often observed overlapping cadherin and β -catenin immunostaining. These results suggest that cadherin–catenin complexes may be involved in stabilizing interactions between SGNs and myocytes; however, it is not possible to conclude that they play a more direct role in synaptic function.

A previous study provided evidence that the structure of cardiac sympathetic synapses is different from the neuromuscular junction and central nervous system synapses (Landis, 1976). Using electron microscopy, Landis (1976) found that in a coculture of cardiac myocytes and SGNs, varicosities containing numerous synaptic vesicles were present along the length of contacting axons. These varicosities were seen 20–30 nm from the myocyte surface but also occurred at greater distances. Analysis of sympathetic and parasympathetic neuromuscular junctions in the guinea pig sinoatrial node revealed neuromuscular separations of ~ 80 nm, which is greater than distances between pre- and postsynaptic membranes in central synapses (Choate et al., 1993). The limit of resolution by a two-photon microscope is ~ 500 nm, which is considerably lower than what is necessary to estimate the distances between pre- and postsynaptic membranes in our studies. Nevertheless, we observed

that the postsynaptic cardiac myocyte membrane develops into specialized zones that invaginate to surround contacting axons. This can be seen in several 3D reconstructions of two-photon images (Figs. 8 E, 9 C, 10 C, and Video 1). The formation of this invagination in the myocyte membrane likely involves remodeling of the cytoskeleton, which might be controlled by cadherin–catenin complexes that accumulate at sites of contact between SGNs and myocytes (Figs. 5 and 6). These specialized zones contain accumulations of β_1 ARs and the scaffold proteins SAP97 and AKAP79/150. The accumulation of scaffold components AKAP79/150 and SAP97 at the postsynaptic zone indicates the formation of a specific signaling domain on the myocyte plasma membrane that may be required for physiologic signaling of ARs in cardiac tissue.

In contrast to SAP97 and AKAP79, caveolin-3 is diminished at sites of myocyte–neuron contact (Fig. 4). Caveolin-3 is a muscle-specific marker of caveolae (a membrane subdomain) that is formed from lipid rafts by the polymerization of caveolins, which are hairpinlike palmitoylated integral membrane proteins that bind cholesterol (Cohen et al., 2004). Caveolae are plasma membrane signaling domains that recruit certain lipid-modified membrane proteins (including receptors, G proteins, and tyrosine kinases) while excluding other proteins and lipid components (Cohen et al., 2004). These distinct plasma membrane domains, synaptic and extrasynaptic, are likely to play important roles in distinguishing receptor signaling in response to catecholamines released from sympathetic nerve terminals (primarily norepinephrine) from catecholamines released from the adrenal gland (primarily epinephrine) and delivered by circulation.

Sympathetic synapses direct the distinct localization of β_1 and β_2 ARs

Acute activation of cardiac β ARs leads to an increase in heart rate and contractility and is an essential component of the physiologic response to stress. However, prolonged activation of cardiac β ARs by the sympathetic nervous system plays a key role in the pathogenesis of heart failure (Mann and Bristow, 2005). Both β_1 and β_2 ARs are expressed in the heart. These two AR subtypes are highly homologous both structurally and functionally. However, these subtypes play distinct roles in regulating normal cardiovascular physiology (Rohrer et al., 1999), and there is a growing body of evidence that they may play opposing roles in the pathogenesis of heart failure (Patterson et al., 2004; Bernstein et al., 2005; Zheng et al., 2005). Our current studies show that the subtype-specific distribution of β_1 and β_2 ARs relative to sympathetic synapses may contribute to the differences in signaling.

Synaptic localization of the β_1 AR. Accumulation of β_1 ARs along with adhesion molecules, adaptor proteins, and signaling molecules suggests a highly organized signaling compartment designed for the most efficient transfer of information from the SGN to the heart. The mechanism for the synaptic localization of β_1 AR is not known. In the postsynaptic density of neuronal excitatory synapses, PDZ proteins organize receptors and their associated signaling proteins and determine the size and strength of synapses (Kim and Sheng, 2004). It has

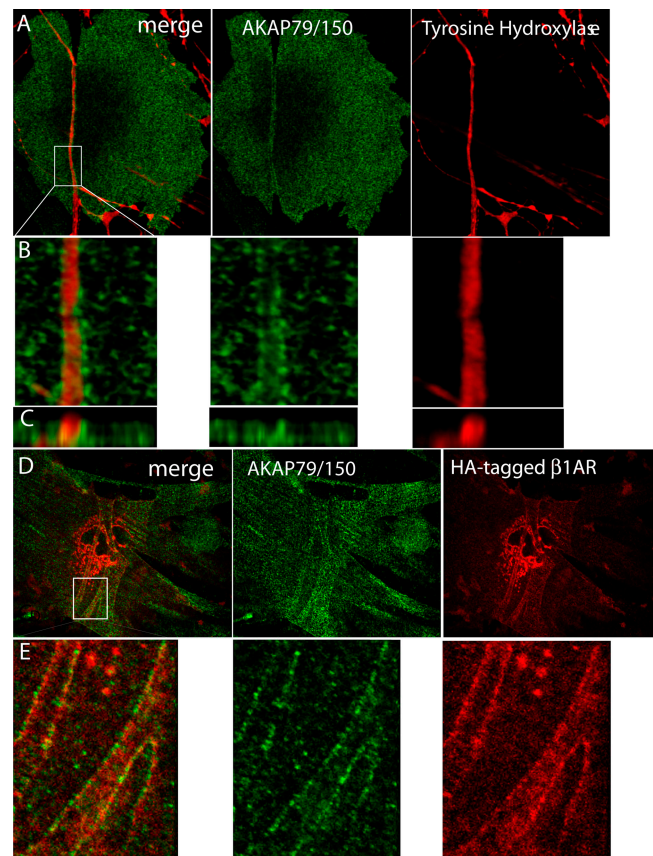


Figure 10. **AKAP79/150 accumulates at cardiac sympathetic synapses in vitro.** (A) Colocalization of AKAP79/150 and tyrosine hydroxylase. Cardiac myocytes and SGNs were cultured for 7 d and immunostained for tyrosine hydroxylase (red) and AKAP79/150 (green); two-photon image. (B) 3D-reconstructed enlarged fragment of the boxed area in A. (C) X-z cross section of the 3D reconstruction. (D) Colocalization of β_1 AR and AKAP79/150. Cardiac myocytes were cocultured with SGNs for 6 d, infected with recombinant adenovirus expressing HA-tagged β_1 AR, and cultured for an additional 24 h before immunostaining for HA (red) and AKAP79/150 (green); two-photon image. (E) 3D-reconstructed enlarged fragment of the boxed area in D.

been shown that the C-terminal PDZ-binding motif of β_1 AR can bind directly to several PDZ domain–containing proteins, including PSD-95, MAGI-2, MAGI-3, ZO-1, GIPC, CAL, and SAP97 (He et al., 2006). Moreover, we have previously shown that disrupting the C-terminal PDZ-binding motif of β_1 AR dramatically alters its signaling in neonatal cardiac myocytes. The wild-type β_1 AR does not undergo agonist-induced internalization in cardiac myocytes and signals only through Gs. In contrast, the β_1 AR-PDZ mutant internalizes upon agonist exposure and couples to both Gs and Gi (Xiang et al., 2002). Thus, PDZ domain interactions are important for normal β_1 AR function. Therefore, we were surprised to find that the synaptic localization of β_1 AR was not disrupted by mutation of its C-terminal PDZ ligand (Fig. 9, C and D). However, for several postsynaptic receptors, including GluR2 (Osten et al., 2000; Chang and Rongo, 2005) and NMDARs (Migaud et al., 1998; Sprengel et al., 1998; Passafaro et al., 1999), it has been shown that synaptic localization is regulated through the sequences outside of the PDZ-binding motif.

It should be noted that we observed only partial colocalization of β_1 AR with SAP97 and AKAP79/150 (Figs. 9 and 10). The partial overlap may represent physiologically relevant interactions, or it may simply be a coincidence of having both proteins localized to the sympathetic synapse. β_1 AR is likely to be only one of several signaling membrane proteins (channels and receptors) at the sympathetic synapse. Sympathetic nerves also release ATP and neuropeptide Y, and the GPCRs recognizing these substances may also be localized to the synapse and could interact with SAP97 and AKAP79/150 in signaling domains that are distinct from the β_1 AR signaling compartment. Thus, SAP97 or AKAP79/150 may be involved in forming signaling compartments with several different GPCRs. It is also possible that we are saturating the β_1 AR signaling compartment with the recombinant adenoviral-expressed HA-tagged β_1 AR. This could explain why not all β_1 ARs localize with SAP97 and AKAP79/150.

Activity-dependent removal of β_2 ARs from the synaptic sites. In cocultures in which the SGNs were not stimulated by nicotine, β_2 ARs were uniformly distributed across the plasma membrane of the majority of myocytes. However, in a small percentage ($\sim 2\%$) of myocytes, β_2 ARs are depleted from zones in contact with neurons. Stimulation of neuronal activity by nicotine induced the rapid (within 5 min) removal of β_2 ARs from sites of contact in the majority of cells (72% cells; Fig. 7, E–H). The results indicate that β_2 AR is removed from the sites of contact upon the release of neurotransmitter from the SGN; thus, the depletion of β_2 ARs from synapses is dependent on neuronal activity. It has been well established that β_2 ARs undergo agonist-induced internalization in cardiac myocytes (Xiang et al., 2002), and this is the most likely mechanism for the redistribution of β_2 AR after the activation of neurons by nicotine. This is consistent with the ability of the β AR antagonist alprenolol to inhibit the depletion of β_2 AR at sites of contact with SGN (Fig. S3).

Evidence from synaptotagmin uptake experiments suggests that synapsin I puncta represent sites of synaptic vesicle release (Fig. 2). Therefore, it is somewhat surprising that β_2 AR depletion is observed along the entire axon (Fig. 7) and not just at synapsin I puncta. This may be caused by the diffusion of neurotransmitter between sites of synaptic vesicle release. Diffusion of neurotransmitter may be facilitated by the greater distance between pre- and postsynaptic membranes in neuroeffector junctions of SGNs and cardiac myocytes compared with central nervous system synapses (Choate et al., 1993). It is also possible that β_2 ARs localized under SGNs are relatively mobile because of the lack of caveolin-3 (Fig. 4) or other interacting proteins. As a result, during the 5 min of SGN stimulation, noninternalized β_2 AR could diffuse to regions of neurotransmitter release. Both explanations are consistent with the finding that β_2 AR depletion was greater under synapsin I puncta compared with regions of the axon between synapsin I puncta (Fig. 7 H).

The redistribution of β_2 AR after the stimulation of neurons suggests that this subtype may exhibit spatially and temporally complex signaling behavior. The response of β_2 AR to noradrenaline released at synapses has to be temporally limited

by internalization. β_2 ARs localized to extrasynaptic sites have limited exposure to high concentrations of norepinephrine but may still respond to epinephrine released from the adrenal gland into the circulation. Thus, the acute stimulation of β_2 ARs localized in the sympathetic synapse may distinctly activate different signaling pathways than the activation of β_2 ARs associated with extrasynaptic caveolin-3 through circulating catecholamines.

Conclusion

We used cocultures of SGNs and cardiac myocytes to study the sympathetic synapse *in vitro*. We have shown that the sympathetic innervation of cardiac myocytes is associated with the formation of distinct plasma membrane signaling domains that are enriched in cadherins, catenins, SAP97, AKAP79, and β_1 ARs and are depleted in caveolin-3. The β_2 ARs exhibit activity-dependent dynamic behavior at the synaptic sites. The distinct plasma membrane domains are likely to play important roles in distinguishing receptor signaling in response to catecholamines released from sympathetic nerve terminals (predominantly norepinephrine) from catecholamines released from the adrenal gland (predominantly epinephrine) and delivered by the circulation. A better understanding of the organization of these signaling complexes will be important for defining the different roles played by these β AR subtypes in normal cardiovascular physiology as well as in the pathogenesis of heart failure.

Materials and methods

Coculture of SGNs and neonatal mouse ventricular myocytes

SGNs were isolated from the cervical ganglia of newborn mouse pups by treating ganglia with collagenase type 1A-S (Sigma-Aldrich) and trypsin T XI (Sigma-Aldrich) followed by trituration. Neurons were plated on coverslips coated with laminin (Sigma-Aldrich) for immunocytochemistry as described previously (Brum et al., 2006). Spontaneously beating neonatal cardiac myocytes were prepared from hearts of newborn mouse pups (from wild-type, β_1 AR KO, β_2 AR KO, and β_1/β_2 AR KO mice) as described previously (Devic et al., 2001) and were added to already plated SGNs on the same day. After coculture for 24 h, cultures were treated with 1 μ M cytosine arabinoside (Sigma-Aldrich) for 24 h to inhibit fibroblast growth. Cocultures were maintained in Leibovitz's L-15 medium supplemented with Nu serum (BD Biosciences), NGF (Invitrogen), and ITS liquid media supplement (Sigma-Aldrich). After cytosine arabinoside treatment, media were changed every 3 d as previously described (Brum et al., 2006).

Infection of cardiac myocytes with recombinant adenovirus

Recombinant adenoviruses encoding HA- β_1 AR and FLAG- β_2 AR were prepared as previously described (Xiang et al., 2002). Cocultures of cardiac myocytes and SGNs were infected with viruses at a multiplicity of infection of 100 at a desired time point (between 1–10 d in culture) and were analyzed 24–72 h later. SGNs are resistant to adenovirus infection, so primarily cardiac myocytes were infected.

Immunofluorescence microscopy

Cocultures were fixed by adding PBS (Mediatech, Inc.) containing 8% PFA directly to the culturing media to achieve a final PFA concentration of 4%. Cells were permeabilized with 1% BSA solution in PBS containing 0.2% Triton X-100. Cells were then stained with the desired antibody. The antibodies used were as follows: anti-FLAG M1 antibody (mouse monoclonal IgG2b; 1:600; Sigma-Aldrich), anti-HA 16b12 antibody (mouse monoclonal IgG1; 1:600; Covance); and rabbit polyclonal; 1:1,000; Berkeley Antibody Company), antisynapsin I (rabbit polyclonal; 1:1,000; Chemicon International), anti-SAP97 (mouse monoclonal; 1:250; StressGen Biotechnologies), anti- β -catenin (mouse monoclonal; 1:300; Transduction Laboratories), antipancadherin (mouse monoclonal; 1:500; Sigma-Aldrich), and antityrosine hydroxylase (rabbit polyclonal; 1:1,000; Chemicon International); and mouse monoclonal; 1:800; Transduction Laboratories). The rabbit polyclonal

antibody to the luminal domain of synaptotagmin I was a gift from P. Scheiffele (Columbia University, New York, NY). The primary antibodies were detected with AlexaFluor594-conjugated goat anti-mouse IgG (1:1,000; Invitrogen) and AlexaFluor488 goat anti-rabbit IgG (1:1,000; Invitrogen). The slices for imaging were mounted with Vectashield mounting media (Vector Laboratories). The images were acquired at room temperature on an imaging microscope (Axioplan 2; Carl Zeiss MicroImaging, Inc.) using a plan-Apochromat 63X 1.40 NA oil lens (Carl Zeiss MicroImaging, Inc.), a camera (RTE/CCD-1300-Y/HS; Roper Scientific), and IPLab software (BD Biosciences). Confocal images were acquired using a confocal laser-scanning microscope (LSM510; Carl Zeiss MicroImaging, Inc.) equipped with a tunable Ti:Sapphire laser (Mira 900; Coherent) and a plan-Apo 63X 1.4 NA oil lens, and images were analyzed by Volocity software (Improvision).

Measurement of the spontaneous contraction rate of myocytes in the functional assay

Measurement of the spontaneous contraction rate was performed as described previously (Devic et al., 2001) with some modifications. In brief, $2-3 \times 10^5$ cardiac cells were cultured on the coverslips coated with laminin (Sigma-Aldrich) and were placed in 35-mm petri dishes (Corning) to obtain a uniformly beating syncytium. SGNs were placed on the same coverslip or on a separate coverslip. On day 10–14, the culture dishes were placed in a temperature regulation apparatus positioned on the stage of an inverted microscope (TMS; Nikon) connected to a video camera (C2400-7; Hamamatsu). Cells were equilibrated at 37°C for 10 min before monitoring the contraction rate. Contraction rates of cells within the syncytium were determined at 60-s intervals for 10 min before and 20 min after the stimulation of SGNs by 1 μ M (–)nicotine hydrogen tartrate salt (Sigma-Aldrich). The data were analyzed using Prizm software (Prizm Software).

Stimulation of SGNs with nicotine

In experiments measuring the beat rate of myocytes cocultured with SGNs, 1 μ M nicotine ([–]nicotine hydrogen tartrate salt; Sigma-Aldrich) was used to avoid activation of the myocytes by outflow of the released transmitter. In all other experiments, 500 μ M nicotine was applied for 5 min followed by washout with prewarmed media.

Quantification of β_2 AR removal from the sites of contact with SGNs

The Volocity program (Improvision) was used to quantify β_2 AR removal from the sites of contact between myocytes with SGNs. Mean fluorescence intensity for the red channel representing immunostaining for FLAG-tagged β_2 AR was measured in areas where the green channel fluorescence (immunostaining for synapsin I) was selected as a criterion. Axonal areas where residual fluorescence for green channel was present were included. Next, we excluded the area selected and measured the mean fluorescence for the red channel at the extrasynaptic regions. Measurements were performed in arbitrary units of a direct scale. Data were collected from 10 images obtained in three experiments.

To compare the fluorescence intensity of β_2 AR staining in the areas of synapsin I accumulation with areas along axons between synapsin I puncta, we used the Wizard tool of the Volocity program to select regions of interest. The data were obtained from three images using six different pairs of regions of interest on each image. Measurements were performed in arbitrary units of the direct scale. Statistic comparisons were performed with a *t* test. Statistical significance was set as $P < 0.05$.

Comparison of the accumulation of β_1 AR in the zones of contact with SGNs

We used the histograms of fluorescence intensity of the original LSM510 files for five different images to quantify the accumulation of β_1 AR in the zones of contact with SGNs. Mean fluorescence intensity was quantified in the areas inside and outside the zones of contact along the selected straight line crossing a zone of contact (Fig. 8 B; two zones from each image). Measurements were performed in arbitrary units of the direct scale. Statistic comparisons were performed with a *t* test. Statistical significance was set as $P < 0.05$.

Colocalization of pancadherin immunostaining with synapsin I

Colocalization of pancadherin immunostaining with synapsin I was quantified using the Volocity program (Improvision). Cadherin puncta were defined as discrete areas where fluorescence intensity was higher than threshold fluorescence in areas outside the sites of contacts. We first measured the total number of cadherin puncta and then measured the number of puncta that had colocalization with synapsin puncta. The percentage of

colocalizing puncta was collected from seven images. Analogously, we measured the total number of synapsin puncta and the number of synapsin puncta that had overlap with cadherin puncta.

FM1-43 imaging

All chemicals were purchased from Sigma-Aldrich unless mentioned otherwise. Cells were cultured on microscopy coverglass (Glaswarenfabrik Karl Hecht KG). After 7 d in culture, cocultures were transferred from medium to an imaging chamber containing 400 μ l Tyrode (150 mM NaCl, 4 mM KCl, 2 mM CaCl₂, 2 mM MgCl₂, 10 mM Hepes, 10 mM glucose, pH 7.35; 310 osmol) supplied with 25 μ g/ml NGF (Invitrogen). After mounting on a microscope (TE-200; Nikon), another 400 μ l Tyrode containing 1 mM nicotine tartrate and 10 μ M FM1-43 was added (load). After a 2-min incubation at room temperature, cells were perfused with the original Tyrode containing 0.1 mM ADVASEP-7 (CyDex, Inc.) at a speed of 1 ml/s for \sim 7 min to wash out FM1-43 remaining on the plasma membrane. The destaining protocol (unload) during the imaging period was as follow: Tyrode for 30 s, 500 μ M nicotine in Tyrode for 120 s, and Tyrode for 60 s.

Fluorescence detection of FM1-43 signals was performed using an inverted epifluorescence microscope (TE-200; Nikon) equipped with a plan Fluor 40X 1.3 NA objective (Nikon). Images were obtained with an intensified CCD camera (XR/Mega-10; Stanford Photonics) operating in gated acquisition mode. The samples were exposed to brief pulses of arc lamp illumination (470/40 nm; Chroma Technology Corp.) via an optical switch (Lambda 10-2; Sutter Instrument Co.). The emission signal was filtered by a 515-nm long-pass optical filter (Chroma Technology Corp.). The imaging rate was 1 Hz, and the exposure time was 30 ms with intensifier gain at 900 V. Images were downloaded in a 10-bit digital format (MV-1465; mTech) and processed with MetaFluor (MicroDevice). Off-line analysis was performed with ImageJ (National Institutes of Health) and Excel software (Microsoft). The data were plotted by SigmaPlot (Systat Software). Each point represents the mean of a total of 55 puncta chosen on a surface of cardiac myocytes from two different cocultures. We normalized fluorescence intensity change within the range of 0 to 1 for each experiment. In addition, regression fitting was used to offset the photobleaching effect. In detail, the fluorescent signal from the images, which was taken during the first 30 s of Tyrode perfusion, was used to generate an exponential decay function. This function was then used to correct the photobleaching of the first 30-s image such that a steady baseline could be established, and its mean fluorescence intensity value was defined as 1. Similarly, the very last 60-s images were used to generate an exponential decay function, which was used to establish a steady baseline (defined as 0). The fluorescence intensity change in between was then subjected to regression fitting based on the two defined exponential decays and was normalized by the defined 1 and 0 baselines.

Immunostaining of mouse cardiac sections

Mice were killed, and hearts were removed and placed in cold PBS buffer. The hearts were rinsed in buffer, cut into halves, and fixed in cold PBS containing 4% PFA for 24 h at 4°C. 50–70- μ m slices were cut by a sectioning system (Series 1000; Vibratome) and incubated in blocking solution for 1 h followed by immunostaining. Imaging was performed by two-photon microscopy using 0.3- μ m slices. 3D reconstruction was performed using Volocity software (Improvision).

Detection of synaptic activity by uptake of the antibody to the luminal domain of synaptotagmin

The antibody to the luminal domain of synaptotagmin (rabbit polyclonal) was a gift from P. Scheiffele. Cocultures of cardiac myocytes and SGNs were incubated with serum-free media containing 500 μ M nicotine and 10 μ g/ml synaptotagmin antibody for 15 min followed by washout with prewarmed complete media. Cells were then fixed and stained with mouse monoclonal to synapsin I.

Online supplemental material

Fig. S1 shows uptake and release of the fluorescent dye FM1-43 by sympathetic neurons innervating cardiac myocytes. Fig. S2 shows immunostaining for β -catenin and synapsin I in the mouse heart. Fig. S3 shows the effect of a β blocker on the removal of β_2 AR from sympathetic synapses. It demonstrates that the pretreatment of coculture with a β blocker abolishes the activity-dependent removal of β_2 AR from synaptic sites. Fig. S4 shows the increase of SAP97 accumulation at the synaptic sites after 90 min of stimulation with nicotine in cocultures in which β_1 AR was overexpressed in cardiac myocytes. Fig. S5 shows immunostaining for SAP97 and synapsin I in the mouse heart. Video 1 shows the rotation of the 3D-reconstructed

image in Fig. 8 E. Online supplemental material is available at <http://www.jcb.org/cgi/content/full/jcb.200604167/DC1>.

We acknowledge Peter Scheiffele for the antibody to the luminal domain of synaptotagmin, Kaman Lee (Stanford Imaging Facility, Stanford, CA) for excellent technical assistance, and Thomas Misgeld (Harvard University, Cambridge, MA) for valuable technical advice.

This work was supported by National Institutes of Health grants 1R01 HL71078-01 (to B.K. Kobilka) and NS40701 (to M.L. Dell'Acqua).

Submitted: 28 April 2006

Accepted: 6 January 2007

References

- Armour, J.A., and J.L. Ardell. 1994. Neurocardiology. Oxford University Press, New York, NY. 443 pp.
- Bamji, S.X., K. Shimazu, N. Kimes, J. Huelsken, W. Birchmeier, B. Lu, and L.F. Reichardt. 2003. Role of beta-catenin in synaptic vesicle localization and presynaptic assembly. *Neuron*. 40:719–731.
- Bauman, A.L., A.S. Goehring, and J.D. Scott. 2004. Orchestration of synaptic plasticity through AKAP signaling complexes. *Neuropharmacology*. 46:299–310.
- Bernstein, D., G. Fajardo, M. Zhao, T. Urashima, J. Powers, G. Berry, and B.K. Kobilka. 2005. Differential cardioprotective/cardiotoxic effects mediated by beta-adrenergic receptor subtypes. *Am. J. Physiol. Heart Circ. Physiol.* 289:H2441–H2449.
- Betz, W.J., and G.S. Bewick. 1992. Optical analysis of synaptic vesicle recycling at the frog neuromuscular junction. *Science*. 255:200–203.
- Bredt, D.S., and R.A. Nicoll. 2003. AMPA receptor trafficking at excitatory synapses. *Neuron*. 40:361–379.
- Brum, P.C., C.M. Hurt, O.G. Shcherbakova, B. Kobilka, and T. Angelotti. 2006. Differential targeting and function of alpha2A and alpha2C adrenergic receptor subtypes in cultured sympathetic neurons. *Neuropharmacology*. 51:397–413.
- Chang, H.C., and C. Rongo. 2005. Cytosolic tail sequences and subunit interactions are critical for synaptic localization of glutamate receptors. *J. Cell Sci.* 118:1945–1956.
- Choate, J.K., M. Klemm, and G.D. Hirst. 1993. Sympathetic and parasympathetic neuromuscular junctions in the guinea-pig sino-atrial node. *J. Auton. Nerv. Syst.* 44:1–15.
- Cohen, A.W., R. Hnasko, W. Schubert, and M.P. Lisanti. 2004. Role of caveolae and caveolins in health and disease. *Physiol. Rev.* 84:1341–1379.
- Dell'Acqua, M.L., K.L. Dodge, S.J. Tavalin, and J.D. Scott. 2002. Mapping the protein phosphatase-2B anchoring site on AKAP79. Binding and inhibition of phosphatase activity are mediated by residues 315–360. *J. Biol. Chem.* 277:48796–48802.
- Devic, E., Y. Xiang, D. Gould, and B. Kobilka. 2001. Beta-adrenergic receptor subtype-specific signaling in cardiac myocytes from beta(1) and beta(2) adrenoceptor knockout mice. *Mol. Pharmacol.* 60:577–583.
- Esler, M., and D. Kaye. 2000. Measurement of sympathetic nervous system activity in heart failure: the role of norepinephrine kinetics. *Heart Fail. Rev.* 5:17–25.
- Funke, L., S. Dakoji, and D.S. Bredt. 2005. Membrane-associated guanylate kinases regulate adhesion and plasticity at cell junctions. *Annu. Rev. Biochem.* 74:219–245.
- Furshpan, E.J., S.C. Landis, S.G. Matsumoto, and D.D. Potter. 1986. Synaptic functions in rat sympathetic neurons in microcultures. I. Secretion of norepinephrine and acetylcholine. *J. Neurosci.* 6:1061–1079.
- Garner, C.C., R.G. Zhai, E.D. Gundelfinger, and N.E. Ziv. 2002. Molecular mechanisms of CNS synaptogenesis. *Trends Neurosci.* 25:243–251.
- Goda, Y., and G.W. Davis. 2003. Mechanisms of synapse assembly and disassembly. *Neuron*. 40:243–264.
- Haass, M., and W. Kubler. 1997. Nicotine and sympathetic neurotransmission. *Cardiovasc. Drugs Ther.* 10:657–665.
- He, J., M. Bellini, H. Inuzuka, J. Xu, Y. Xiong, X. Yang, A.M. Castleberry, and R.A. Hall. 2006. Proteomic analysis of beta1-adrenergic receptor interactions with PDZ scaffold proteins. *J. Biol. Chem.* 281:2820–2827.
- Kim, E., and M. Sheng. 2004. PDZ domain proteins of synapses. *Nat. Rev. Neurosci.* 5:771–781.
- Kraszewski, K., O. Mundigl, L. Daniell, C. Verderio, M. Matteoli, and P. De Camilli. 1995. Synaptic vesicle dynamics in living cultured hippocampal neurons visualized with CY3-conjugated antibodies directed against the luminal domain of synaptotagmin. *J. Neurosci.* 15:4328–4342.
- Landis, S.C. 1976. Rat sympathetic neurons and cardiac myocytes developing in microcultures: correlation of the fine structure of endings with neurotransmitter function in single neurons. *Proc. Natl. Acad. Sci. USA.* 73:4220–4224.
- Lechner, S.G., M. Mayer, and S. Boehm. 2003. Activation of M1 muscarinic receptors triggers transmitter release from rat sympathetic neurons through an inhibition of M-type K⁺ channels. *J. Physiol.* 553:789–802.
- Mann, D.L., and M.R. Bristow. 2005. Mechanisms and models in heart failure: the biomechanical model and beyond. *Circulation*. 111:2837–2849.
- Migaud, M., P. Charlesworth, M. Dempster, L.C. Webster, A.M. Watabe, M. Makhinson, Y. He, M.F. Ramsay, R.G. Morris, J.H. Morrison, T.J. O'Dell, and S.G. Grant. 1998. Enhanced long-term potentiation and impaired learning in mice with mutant postsynaptic density-95 protein. *Nature*. 396:433–439.
- Misgeld, T., R.W. Burgess, R.M. Lewis, J.M. Cunningham, J.W. Lichtman, and J.R. Sanes. 2002. Roles of neurotransmitter in synapse formation: development of neuromuscular junctions lacking choline acetyltransferase. *Neuron*. 36:635–648.
- Muller, B.M., U. Kistner, R.W. Veh, C. Cases-Langhoff, B. Becker, E.D. Gundelfinger, and C.C. Garner. 1995. Molecular characterization and spatial distribution of SAP97, a novel presynaptic protein homologous to SAP90 and the *Drosophila* discs-large tumor suppressor protein. *J. Neurosci.* 15:2354–2366.
- Norenberg, W., I. Gobel, A. Meyer, S.L. Cox, K. Starke, and A.U. Trendelenburg. 2001. Stimulation of mouse cultured sympathetic neurons by uracil but not adenine nucleotides. *Neuroscience*. 103:227–236.
- Osten, P., L. Khatri, J.L. Perez, G. Kohr, G. Giese, C. Daly, T.W. Schulz, A. Wensky, L.M. Lee, and E.B. Ziff. 2000. Mutagenesis reveals a role for ABP/GRIP binding to GluR2 in synaptic surface accumulation of the AMPA receptor. *Neuron*. 27:313–325.
- Park, M., E.C. Penick, J.G. Edwards, J.A. Kauer, and M.D. Ehlers. 2004. Recycling endosomes supply AMPA receptors for LTP. *Science*. 305:1972–1975.
- Passafaro, M., C. Sala, M. Niethammer, and M. Sheng. 1999. Microtubule binding by CRIPT and its potential role in the synaptic clustering of PSD-95. *Nat. Neurosci.* 2:1063–1069.
- Patterson, A.J., W. Zhu, A. Chow, R. Agrawal, J. Kosek, R.P. Xiao, and B. Kobilka. 2004. Protecting the myocardium: a role for the beta2 adrenergic receptor in the heart. *Crit. Care Med.* 32:1041–1048.
- Perez-Otano, I., and M.D. Ehlers. 2005. Homeostatic plasticity and NMDA receptor trafficking. *Trends Neurosci.* 28:229–238.
- Perkins, G.A., L. Wang, L.J. Huang, K. Humphries, V.J. Yao, M. Martone, T.J. Deerinck, D.M. Barraclough, J.D. Violin, D. Smith, et al. 2001. PKA, PKC, and AKAP localization in and around the neuromuscular junction. *BMC Neurosci.* 2:17.
- Potter, D.D., S.C. Landis, S.G. Matsumoto, and E.J. Furshpan. 1986. Synaptic functions in rat sympathetic neurons in microcultures. II. Adrenergic/cholinergic dual status and plasticity. *J. Neurosci.* 6:1080–1098.
- Rohrer, D.K., A. Chruscinski, E.H. Schauble, D. Bernstein, and B.K. Kobilka. 1999. Cardiovascular and metabolic alterations in mice lacking both beta1- and beta2-adrenergic receptors. *J. Biol. Chem.* 274:16701–16708.
- Ryan, T.A., H. Reuter, B. Wendland, F.E. Schweizer, R.W. Tsien, and S.J. Smith. 1993. The kinetics of synaptic vesicle recycling measured at single presynaptic boutons. *Neuron*. 11:713–724.
- Rybin, V.O., X. Xu, M.P. Lisanti, and S.F. Steinberg. 2000. Differential targeting of beta-adrenergic receptor subtypes and adenylyl cyclase to cardiomyocyte caveolae. A mechanism to functionally regulate the cAMP signaling pathway. *J. Biol. Chem.* 275:41447–41457.
- Sanes, J.R., and J.W. Lichtman. 1999. Development of the vertebrate neuromuscular junction. *Annu. Rev. Neurosci.* 22:389–442.
- Sanes, J.R., and J.W. Lichtman. 2001. Induction, assembly, maturation and maintenance of a postsynaptic apparatus. *Nat. Rev. Neurosci.* 2:791–805.
- Scheiffele, P., J. Fan, J. Choih, R. Fetter, and T. Serafini. 2000. Neuroligin expressed in nonneuronal cells triggers presynaptic development in contacting axons. *Cell*. 101:657–669.
- Sheng, M., and M.J. Kim. 2002. Postsynaptic signaling and plasticity mechanisms. *Science*. 298:776–780.
- Shenoy, S.K., and R.J. Lefkowitz. 2003. Multifaceted roles of beta-arrestins in the regulation of seven-membrane-spanning receptor trafficking and signalling. *Biochem. J.* 375:503–515.
- Sprengel, R., S.B. Amico, C. Brusa, R. Burnashev, N. Rozov, A. Hvalby, O. Jensen, V. Paulsen, O. Andersen, P. Kim, et al. 1998. Importance of the intracellular domain of NR2 subunits for NMDA receptor function in vivo. *Cell*. 92:279–289.
- Sudhof, T.C. 2001. alpha-Latrotoxin and its receptors: neuroligins and CIRL/latrophilins. *Annu. Rev. Neurosci.* 24:933–962.

- Valenzuela, D.M., T.N. Stitt, P.S. DiStefano, E. Rojas, K. Mattsson, D.L. Compton, L. Nunez, J.S. Park, J.L. Stark, D.R. Gies, et al. 1995. Receptor tyrosine kinase specific for the skeletal muscle lineage: expression in embryonic muscle, at the neuromuscular junction, and after injury. *Neuron*. 15:573–584.
- von Zastrow, M., and B.K. Kobilka. 1992. Ligand-regulated internalization and recycling of human beta 2-adrenergic receptors between the plasma membrane and endosomes containing transferrin receptors. *J. Biol. Chem.* 267:3530–3538.
- Xiang, Y., and B. Kobilka. 2003a. The PDZ-binding motif of the beta2-adrenoceptor is essential for physiologic signaling and trafficking in cardiac myocytes. *Proc. Natl. Acad. Sci. USA*. 100:10776–10781.
- Xiang, Y., and B.K. Kobilka. 2003b. Myocyte adrenoceptor signaling pathways. *Science*. 300:1530–1532.
- Xiang, Y., E. Devic, and B. Kobilka. 2002. The PDZ binding motif of the beta 1 adrenergic receptor modulates receptor trafficking and signaling in cardiac myocytes. *J. Biol. Chem.* 277:33783–33790.
- Xiang, Y., F. Naro, M. Zoudilova, S.L. Jin, M. Conti, and B. Kobilka. 2005. Phosphodiesterase 4D is required for beta2 adrenoceptor subtype-specific signaling in cardiac myocytes. *Proc. Natl. Acad. Sci. USA*. 102:909–914.
- Xiao, R.P., W. Zhu, M. Zheng, K. Chakir, R. Bond, E.G. Lakatta, and H. Cheng. 2004. Subtype-specific beta-adrenoceptor signaling pathways in the heart and their potential clinical implications. *Trends Pharmacol. Sci.* 25:358–365.
- Yamagata, M., J.R. Sanes, and J.A. Weiner. 2003. Synaptic adhesion molecules. *Curr. Opin. Cell Biol.* 15:621–632.
- Yang, B., J.D. Slonimsky, and S.J. Birren. 2002. A rapid switch in sympathetic neurotransmitter release properties mediated by the p75 receptor. *Nat. Neurosci.* 5:539–545.
- Zakharenko, S.S., L. Zablow, and S.A. Siegelbaum. 2001. Visualization of changes in presynaptic function during long-term synaptic plasticity. *Nat. Neurosci.* 4:711–717.
- Zheng, M., W. Zhu, Q. Han, and R.P. Xiao. 2005. Emerging concepts and therapeutic implications of beta-adrenergic receptor subtype signaling. *Pharmacol. Ther.* 108:257–268.